

Configurations of Solvated Complex Ions of First Transition Metals in Hexamethylphosphoric Triamide as Inferred from Their Absorption Spectra and Stokes Radii

Yuriko ABE* and Goro WADA

Department of Chemistry, Nara Women's University, Nara 630

(Received April 10, 1980)

The absorption spectra and Stokes radii of solvated complex ions of first transition metals (Mn(II), Fe(II), Co(II), Ni(II), Cu(II), and Zn(II)) were observed in hexamethylphosphoric triamide (HMPA) in order to determine their configurations. It seems that the Stokes radii of complex ions are sensitive to the configurational change, since the diameter of an HMPA molecule is very large as compared with the crystallographic diameters of central metal ions. As to the result, metal ions are tetrahedrally solvated in the cases of Mn(II), Fe(II), Co(II), and Cu(II), while in the case of Ni(II), equilibria are established among octahedral, square planar and tetrahedral solvated species. Zn(II) forms probably a complex ion solvated octahedrally by HMPA.

Syntheses of the transition metal complexes with hexamethylphosphoric triamide (HMPA), and their solid state stereochemistries have been investigated by many workers.¹⁾ In these solid complexes HMPA tends to form tetrahedral configuration around metal ions, when anions such as ClO_4^- , $\text{B}(\text{C}_6\text{H}_5)_4^-$, SCN^- , NO_3^- , SO_4^{2-} , and halide ions, are outside of the coordination sphere, or when some of them are in the coordination sphere as unidentate ligands.¹⁻⁴⁾ But when metal ions are coordinated with anions such as NO_3^- , SO_4^{2-} , and CH_3COO^- ions as multidentate ligands, octahedral or square planar configurations are mostly preferred according to the nature of metal ions.^{1,4)} On the other hand, in nitromethane solution,^{2,3,5)} the complexes $[\text{M}^{\text{II}}(\text{hmpa})_4](\text{ClO}_4)_2$ formed are mostly tetrahedral when M^{II} is Mn^{II} , Fe^{II} , Co^{II} , Cu^{II} , or Zn^{II} , but not so when it is Ni^{II} .

In HMPA solutions, the stereochemistry of the solvated complex ions of the first transition metals has not been reported yet except for the case of Co(II).⁶⁾ In the present study, the absorption spectra and Stokes radii of solvated complex ions of the first transition metals in HMPA were observed in order to determine their configurations. It seems that the Stokes radii are sensitive to the configurational change of solvated complex ions, since the diameter of an HMPA molecule is very large as compared with the crystallographic radii of the central metal ions.

Experimental

Materials. Commercial HMPA of guaranteed reagent grade was distilled under a reduced nitrogen atmosphere of 3 mmHg at 70–80 °C after it had been dried over barium oxide and a small amount of peroxide accidentally contained in HMPA had been decomposed by iron(II) chloride. The distilled HMPA was deoxygenated by passing nitrogen, and then stored in a dark and cool room. Nitromethane was dried over calcium chloride and distilled under atmospheric pressure. Complexes of various metal ions $[\text{M}^{\text{II}}(\text{hmpa})_4](\text{ClO}_4)_2$ ($\text{M}^{\text{II}} = \text{Mn}^{\text{II}}$, Fe^{II} , Co^{II} , Ni^{II} , Cu^{II} , or Zn^{II}) were synthesized according to the methods reported by Donoghue and Drago.^{2,3)} Stock solutions of these metal complexes were prepared, and portions of them were used for the spectrophotometric or conductivity determinations. Anhydrous sodium perchlorate was prepared by heating monohydrated salt which had been recrystallized twice from water.

Procedure. For the determination of absorption spectra, a Hitachi Recording Spectrophotometer Model EPS-3T was used with a thermostated cell. The metal ion concentrations in stock solutions were determined spectrophotometrically by the following methods; Mn(II): formaldoxime method⁷⁾ (molar absorptivity $\epsilon = 1.040 \times 10^4 \text{ M}^{-1} \text{ cm}^{-1}$ at 450 nm); Fe(II): 2,2'-bipyridine method⁸⁾ ($\epsilon = 9.205 \times 10^3 \text{ M}^{-1} \text{ cm}^{-1}$ at 522 nm); Co(II): nitroso-R salt method⁹⁾ ($\epsilon = 9.350 \times 10^3 \text{ M}^{-1} \text{ cm}^{-1}$ at 550 nm); Ni(II): dimethylglyoxime method⁸⁾ ($\epsilon = 1.457 \times 10^4 \text{ M}^{-1} \text{ cm}^{-1}$ at 450 nm); Cu(II): sodium diethyldithiocarbamate method⁸⁾ ($\epsilon = 9.223 \times 10^3 \text{ M}^{-1} \text{ cm}^{-1}$ at 430 nm); Zn(II): zincone method⁷⁾ ($\epsilon = 2.341 \times 10^4 \text{ M}^{-1} \text{ cm}^{-1}$ at 620 nm). (1 M = 1 mol dm⁻³.)

The measurements of electric conductivities of HMPA solutions containing complex ions were performed with a Yanagimoto Conductivity Apparatus Model MY-8. The cell used was calibrated with a 0.01 M aqueous KCl solution.

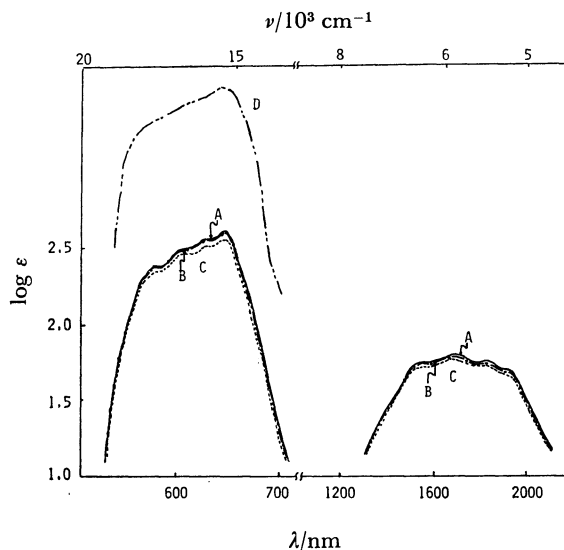


Fig. 1. Absorption spectra of solvated Co^{2+} ion in HMPA and $[\text{Co}(\text{hmpa})_4]^{2+}$ ion in nitromethane at 25 °C.

A(—): $[\text{Co}(\text{hmpa})_4]^{2+} = 8.0 \times 10^{-4} \text{ M}$ in HMPA, B(---): $[\text{Co}(\text{hmpa})_4]^{2+} = 8.0 \times 10^{-4} \text{ M}$ and $[\text{HMPA}]_0 = 0.5 \text{ M}$ in nitromethane, C(....): $[\text{Co}(\text{hmpa})_4]^{2+} = 8.0 \times 10^{-4} \text{ M}$ in nitromethane,²⁾ D(-.-.-): the solid reflectance spectrum²⁾ of $[\text{Co}(\text{hmpa})_4](\text{ClO}_4)_2$, ordinate in arbitrary scale.

Results

The absorption spectra of the solvated Co^{2+} ion in HMPA, and $[\text{Co}(\text{hmpa})_4]^{2+}$ in nitromethane are shown in Fig. 1. Figure 2 shows the absorption spectra of solvated Ni^{2+} ion, which change remarkably with temperature. The absorption spectra of the solvated Cu^{2+} ion in HMPA, and $[\text{Cu}(\text{hmpa})_4]^{2+}$ in nitromethane are shown in Fig. 3.

The plots of the equivalent conductivities of various

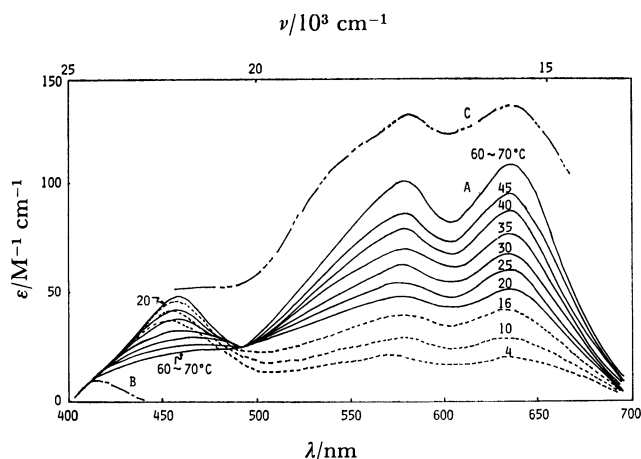


Fig. 2. Absorption spectra of solvated Ni^{2+} ion in HMPA at various temperatures.

A(— and ———): $[\text{Ni}(\text{II})] = 4.1 \times 10^{-3} \text{ M}$ in HMPA, B(—): $[\text{Ni}(\text{dmsO})_6]^{2+} = 4.1 \times 10^{-3} \text{ M}$ in DMSO, C(—): the solid reflectance spectrum²⁾ of $[\text{Ni}(\text{hmpa})_4](\text{ClO}_4)_2$, ordinate in arbitrary scale.

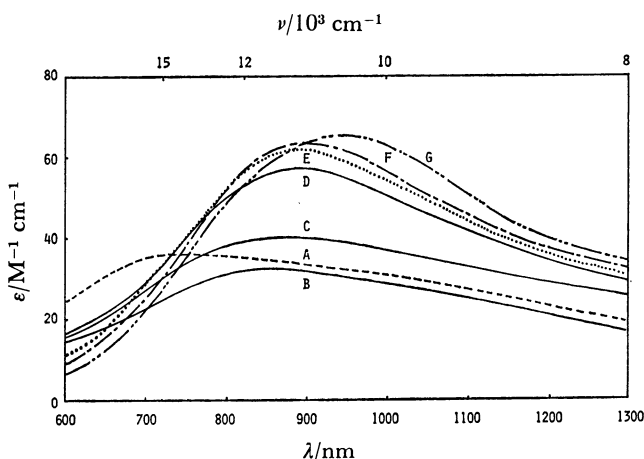


Fig. 3. Absorption spectra of solvated Cu^{2+} ion in HMPA and $[\text{Cu}(\text{hmpa})_4]^{2+}$ ion in nitromethane.

A(—): $[\text{Cu}(\text{hmpa})_4]^{2+} = 2.0 \times 10^{-3} \text{ M}$ in nitromethane, B(—): $[\text{Cu}(\text{hmpa})_4]^{2+} = 2.0 \times 10^{-3} \text{ M}$ and $[\text{HMPA}]_0 = 1.0 \times 10^{-2} \text{ M}$ in nitromethane, C(—): $[\text{Cu}(\text{hmpa})_4]^{2+} = 2.0 \times 10^{-3} \text{ M}$ and $[\text{HMPA}]_0 = 1.0 \times 10^{-1} \text{ M}$ in nitromethane, D(—): $[\text{Cu}(\text{hmpa})_4]^{2+} = 2.0 \times 10^{-3} \text{ M}$ and $[\text{HMPA}]_0 = 5.0 \times 10^{-1} \text{ M}$ in nitromethane, E(—): $[\text{Cu}(\text{hmpa})_4]^{2+} = 2.0 \times 10^{-3} \text{ M}$ and $[\text{HMPA}]_0 = 1.0 \text{ M}$ in nitromethane, F(—): $[\text{Cu}(\text{hmpa})_4]^{2+} = 2.0 \times 10^{-3} \text{ M}$ and $[\text{HMPA}]_0 = 2.0 \text{ M}$ in nitromethane, G(—): $[\text{Cu}(\text{hmpa})_4]^{2+} = 2.0 \times 10^{-3} \text{ M}$ in HMPA (5.8 M).

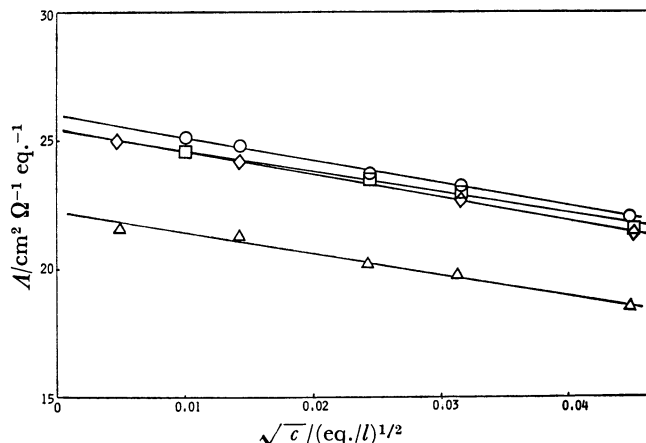


Fig. 4. Relationships of equivalent conductivities of complex perchlorates vs. square roots of equivalent concentrations in HMPA at 25 °C.

◇: Solvated Co^{2+} ion, ○: solvated Fe^{2+} ion, □: solvated Cu^{2+} ion, △: solvated Zn^{2+} ion.

complex perchlorates in HMPA (A) against the square roots of the equivalent concentrations (\sqrt{c}) give straight lines with negative slopes as shown in Fig. 4. Consequently, Eq. 1 holds for these salts;

$$A = A_0 - k\sqrt{c}, \quad (1)$$

where A_0 is a limiting equivalent conductivity and k is an empirical constant. The limiting equivalent ionic conductivity of a solvated cation (λ_0^+) is obtained by subtracting that of perchlorate ion ($\lambda_0^- = 15.5 \text{ cm}^2 \Omega^{-1} \text{ eq.}^{-1}$)⁹⁾ from A_0 . Then, the Stokes radius of the solvated cation (r^+) can be calculated by Eq. 2:

$$r^+ = \frac{0.82|z|}{\lambda_0^+ \eta} \quad (2)$$

where η is the viscosity of HMPA ($\eta = 0.0323$ poise at 25 °C)^{10,11)} and z is the number of electric charges on the solvated cation ($z = 2$). The values of A_0 , λ_0^+ , and r^+ thus obtained are listed in Table 1.

TABLE 1. LIMITING EQUIVALENT CONDUCTIVITIES AND STOKES RADII OF SOLVATED METAL IONS IN HMPA AT 25 °C

Ion	$A_0^a)$ $\text{cm}^2 \Omega^{-1} \text{ eq.}^{-1}$	λ_0^+ $\text{cm}^2 \Omega^{-1} \text{ eq.}^{-1}$	Stokes radius r^+ Å
Mn^{2+}	24.80	9.30	5.47
Fe^{2+}	25.65	10.15	5.00
Co^{2+}	25.58	10.08	5.03
Ni^{2+}	23.40	7.90	6.43
Cu^{2+}	25.31	9.81	5.17
Zn^{2+}	22.20	6.70	7.59

a) Values for complex perchlorates.

Discussion

Configuration of Solvated Co^{2+} Ion in HMPA. In Fig. 1 are shown the absorption spectra of solvated Co^{2+} ion in pure HMPA (Curve A) and of $[\text{Co}(\text{hmpa})_4]^{2+}$ in nitromethane at $[\text{Co}(\text{hmpa})_4]^{2+} = 8.0 \times 10^{-4} \text{ M}$ and $[\text{HMPA}]_0 = 0.5 \text{ M}$ (Curve B). The

latter absorption spectrum is in good agreement with that obtained in nitromethane by Donoghue and Drago,²⁾ which is also shown (Curve C) in Fig. 1. These three spectral patterns are similar to that of the solid reflectance spectrum of $[\text{Co}(\text{hmpa})_4](\text{ClO}_4)_2$ (Curve D), which was reported to be tetrahedral.²⁾ Therefore, it can be reasonably deduced that the solvated Co^{2+} ion in HMPA is regularly tetrahedral.

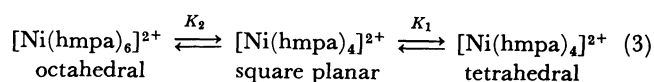
In general,¹²⁾ the absorption bands due to $\nu_2(^4T_1(F) \leftarrow ^4A_2)$ and $\nu_3(^4T_1(P) \leftarrow ^4A_2)$ transitions of tetrahedral cobalt(II) complexes appear in the near-infrared and visible regions, respectively. The molar absorptivities of these bands are of the magnitude of $10\text{--}100 \text{ M}^{-1} \text{ cm}^{-1}$ for ν_2 and $100\text{--}2000 \text{ M}^{-1} \text{ cm}^{-1}$ for ν_3 , respectively. But bands of octahedral cobalt(II) complexes such as $[\text{Co}(\text{H}_2\text{O})_6]^{2+}$, $[\text{Co}(\text{dmso})_6]^{2+}$, $[\text{Co}(\text{pyo})_6]^{2+}$ (pyo = pyridine oxide), and $[\text{Co}(\text{NH}_3)_6]^{2+}$ are observed in the visible region near 500 nm ($\epsilon = 5\text{--}40 \text{ M}^{-1} \text{ cm}^{-1}$). These bands allow a fairly clear-cut distinction between tetrahedral and octahedral cobalt(II) complexes. Thus, the characteristics of the absorption spectrum of solvated Co^{2+} ion in HMPA coincide with those of the tetrahedral $\text{Co}(\text{II})$ complexes. Moreover, the absorption spectrum in HMPA is not affected by temperature. Therefore, it is deduced that no tetrahedral \leftrightarrow octahedral configurational transition of the complex ion exists. Accordingly, it is concluded that the only solvated Co^{2+} ion in HMPA is the tetrahedral $[\text{Co}(\text{hmpa})_4]^{2+}$ ion.

The conductivity measurements of HMPA solutions containing $[\text{Co}(\text{hmpa})_4]^{2+}$ in the concentration range $10^{-5}\text{--}10^{-3} \text{ M}$ give the linear relationships as shown in Fig. 4. This shows clearly that $[\text{Co}(\text{hmpa})_4]^{2+}$ in HMPA forms no ion-pair, because no deviation from the linearity is seen to occur. The perchlorates $[\text{M}^{\text{II}}(\text{hmpa})_4](\text{ClO}_4)_2$ of other first transition metals also dissociate completely in HMPA.

The value of the Stokes radius (r^+) of tetrahedral $[\text{Co}(\text{hmpa})_4]^{2+}$ ion was found to be 5.03 \AA . Since an HMPA molecule coordinated to a divalent metal ion is very bulky as compared with the central metal ion, small differences of the crystallographic radii among the divalent metal ions would have little influence on the Stokes radii of the complexes $[\text{M}^{\text{II}}(\text{hmpa})_4]^{2+}$. Accordingly, when HMPA molecules are tetrahedrally coordinated to the metal ions, it will be reasonable to assume that the values of their Stokes radii are all about 5 \AA , irrespective of the kind of the central metal ions.

Configuration of Solvated Ni^{2+} Ion in HMPA.

Figure 2 shows the temperature dependence of the absorption spectra of solvated Ni^{2+} ion in HMPA. The spectral change is no longer observed above 60°C and the final spectrum agrees very closely with that of the solid reflectance spectrum of the tetrahedral $[\text{Ni}(\text{hmpa})_4](\text{ClO}_4)_2$.²⁾ Since an isosbestic point appears at 490 nm above 20°C , the solvated Ni^{2+} ion is supposed to be in equilibrium between two different configurations in HMPA. At $60\text{--}70^\circ \text{C}$, the solvated Ni^{2+} ions are completely tetrahedral. Below 20°C , the spectra do not pass through the isosbestic point which appears above 20°C but approach to that of the octahedral $[\text{Ni}(\text{dmso})_6]^{2+}$.¹²⁾ Accordingly, the following equilibria seem to exist.



The value of ΔH_1 of the reaction from the square planar to tetrahedral configuration is obtained by Eq. 4;

$$\frac{d \ln K_1}{d T^{-1}} = d \ln \frac{c\Delta\epsilon - \Delta A}{\Delta A} / d T^{-1} = - \frac{\Delta H_1}{R} \quad (4)$$

$$\Delta\epsilon = \epsilon_t^{633} - \epsilon_p^{633}$$

$$\Delta A = A_t - A$$

in which $\epsilon_t^{633} (= 106 \text{ M}^{-1} \text{ cm}^{-1})$ and ϵ_p^{633} stand for the molar absorptivities of the tetrahedral and square planar complexes at 633 nm , respectively, A_t and A are absorbances at $60\text{--}70^\circ \text{C}$ and at a certain temperature between 20°C and 60°C at 633 nm , respectively, and c is total concentration of $\text{Ni}(\text{II})$.

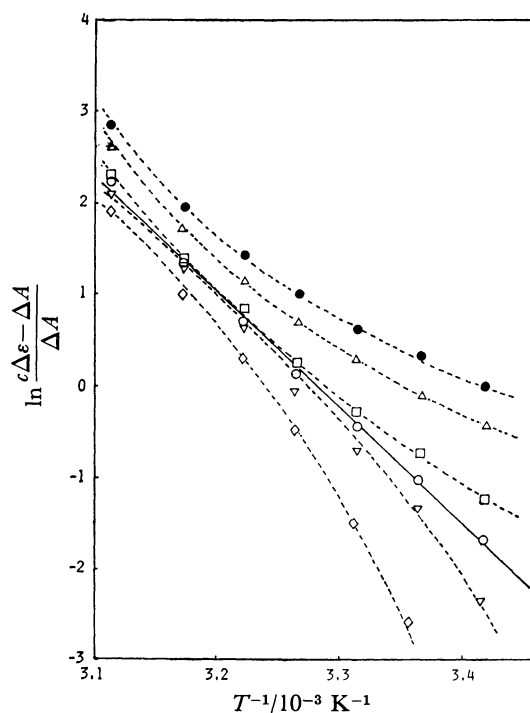


Fig. 5. The plots of $\ln \frac{c\Delta\epsilon - \Delta A}{\Delta A}$ vs. T^{-1} with various

values for ϵ_p^{633} .
 ϵ_p^{633} : ●; $0 \text{ M}^{-1} \text{ cm}^{-1}$, △; $20 \text{ M}^{-1} \text{ cm}^{-1}$,
 □; $40 \text{ M}^{-1} \text{ cm}^{-1}$, ○; $45 \text{ M}^{-1} \text{ cm}^{-1}$,
 ◇; $50 \text{ M}^{-1} \text{ cm}^{-1}$, ◇; $60 \text{ M}^{-1} \text{ cm}^{-1}$.

Figure 5 shows the linear relationship between $\ln[(c\Delta\epsilon - \Delta A)/\Delta A]$ vs. T^{-1} according to Eq. 4. When $\epsilon_p^{633} = 45 \text{ M}^{-1} \text{ cm}^{-1}$ is used, a straight line which satisfies Eq. 4 best can be drawn. Thus, the following results are obtained: $\Delta H_1 = 25.1 \text{ kcal mol}^{-1}$, $\Delta S_1 = 83 \text{ cal K}^{-1} \text{ mol}^{-1}$, and $\Delta G_1 = 0.6 \text{ kcal mol}^{-1}$ at 25°C ($1 \text{ cal} = 4.2 \text{ J}$).

The value of ΔH_2 for the reaction from the octahedral to the square planar configuration is obtained by Eq. 5;

$$\begin{aligned} \frac{d \ln K_2}{d T^{-1}} &= d \ln \frac{-(c\epsilon_o^{633} - A)}{K_1(c\epsilon_t^{633} - A) + (c\epsilon_p^{633} - A)} / d T^{-1} \\ &= - \frac{\Delta H_2}{R} \end{aligned} \quad (5)$$

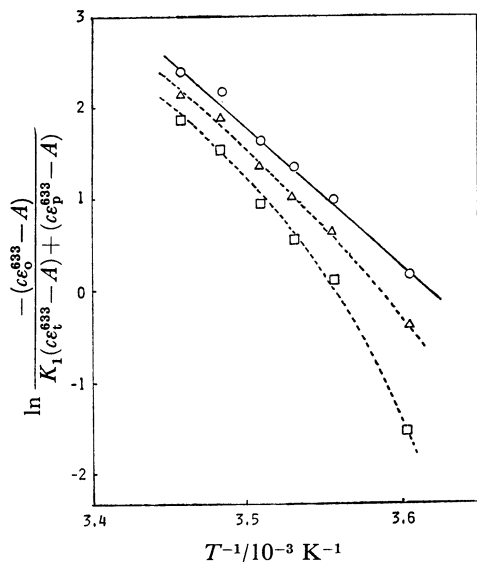


Fig. 6. The plots of $\ln \frac{K_1(\epsilon_o^{633} - A)}{K_1(\epsilon_o^{633} - A) + (\epsilon_p^{633} - A)}$ vs. $1/T$ with various values for ϵ_o^{633} .
 ϵ_o^{633} : ○; 0 M⁻¹ cm⁻¹, △; 10 M⁻¹ cm⁻¹,
 □; 20 M⁻¹ cm⁻¹.

where ϵ_o^{633} is the molar absorptivity of the octahedral configuration at 633 nm. A value $\epsilon_o^{633} = 0$ M⁻¹ cm⁻¹ satisfies Eq. 5 best as shown in Fig. 6. Therefore, the thermodynamic functions are obtained as follows: $\Delta H_2 = 27.8$ kcal mol⁻¹, $\Delta S_2 = 101$ cal K⁻¹ mol⁻¹, and $\Delta G_2 = 0.8$ kcal mol⁻¹ at 25 °C.

In general,¹²⁾ tetrahedral Ni(II) complexes exhibit a visible band near 600–700 nm (ϵ : 100–200 M⁻¹ cm⁻¹) assignable to ${}^3T_1(P) \leftarrow {}^3T_1(\nu_3)$ transition and a near-infrared band near 1250 nm (ϵ : 20 M⁻¹ cm⁻¹) assignable to ${}^3A_2 \leftarrow {}^3T_1(\nu_2)$ transition. On the other hand, octahedral Ni(II) complexes exhibit visible absorption bands of lower molar absorptivities, (ϵ : about 1–10 M⁻¹ cm⁻¹), while square planar Ni(II) complexes show stronger bands in the visible region (ϵ : 50–500 M⁻¹ cm⁻¹). Consequently, the spectral patterns of the tetrahedral, square planar and octahedral complexes observed are quite reasonable ones, and support the explanation of the solution equilibria proposed above.

The Stokes radius of the solvated Ni²⁺ ion in HMPA is 6.43 Å at 25 °C, at which temperature, the equilibrium of the solvated Ni²⁺ ion between the square planar and tetrahedral configurations is established. Since ΔS_1 value of this reaction is a large positive one, the tetrahedral complex seems to be less strongly solvated than the square planar complex is, although the coordination numbers of both complexes are the same. This may be the reason why the average value of the Stokes radius of solvated Ni²⁺ ion in HMPA at 25 °C is larger than 5 Å expected from the tetrahedral configuration.

ΔS_2 value for the reaction from the octahedral to square planar configuration is a larger positive one than that observed in a similar reaction from the octahedral to square planar configuration,¹³⁾ since the HMPA molecules are so closely packed in the coordination sphere of the octahedral complex that the rotational degree of freedom of HMPA is much reduced.

Configuration of Solvated Cu²⁺ Ion in HMPA. A broad absorption maximum near 720 nm in the spectrum at $[[\text{Cu}(\text{hmpa})_4]^{2+}] = 2.0 \times 10^{-3}$ M in nitromethane (Curve A) agrees with that obtained by Donoghue and Drago²⁾ in Fig. 3. In nitromethane at $[\text{HMPA}]_0 = 1.0 \times 10^{-2}$ M (Curve B), the absorption maximum appears near 850 nm and its peak is lower than that in pure nitromethane. In the $[\text{HMPA}]_0$ range 0.1–0.5 M, the absorption maxima shift to longer wavelength, and their peaks become higher (Curves C and D). In nitromethane of the $[\text{HMPA}]_0$ range 1.0–2.0 M and in pure HMPA (5.8 M), the absorption spectra shift further to longer wavelength with only slight absorbance changes (Curves E, F, and G).

In nitromethane, $[\text{Cu}(\text{hmpa})_4]^{2+}$ is square planar because its absorption spectrum resembles that¹⁴⁾ of square planar $[\text{Cu}(\text{Ph}_3\text{PO})_4]^{2+}$. When a small amount of HMPA is added to nitromethane, the Cu(II) complex in the solution seems to become tetragonal with HMPA molecules coordinated along the z axis of the square planar complex. The changes in the absorption spectra in the $[\text{HMPA}]_0$ range 0.1–0.5 M suggest that a tetragonal \leftrightarrow distorted tetrahedral transition is in equilibrium, and that the changes in the solvent properties due to excess HMPA merely shift this equilibrium. According to Wayland and Drago,⁵⁾ the NMR contact shifts are independent of HMPA concentrations in the $[\text{HMPA}]_0$ range 0.5–1.5 M. Consequently, $[\text{Cu}(\text{hmpa})_4]^{2+}$ becomes only distorted tetrahedral at $[\text{HMPA}]_0 = 1.0$ M. In nitromethane of the HMPA concentrations higher than 1.0 M and in pure HMPA, it seems that the change in the absorption spectrum is not due to the change in the coordination number or in the configuration, but due to that in the degree of distortion of the complex. Liehr theoretically predicted¹⁵⁾ that regularly tetrahedral Cu(II) complexes would show an electronic transition in the near-infrared region but not in the visible one. Accordingly, the distorted tetrahedral $[\text{Cu}(\text{hmpa})_4]^{2+}$ at $[\text{HMPA}]_0 = 1.0$ M is gradually liberated from distortion at the HMPA concentrations higher than 1.0 M in nitromethane and finally becoming nearly regular tetrahedral in pure HMPA (5.8 M). The Stokes radius of $[\text{Cu}(\text{hmpa})_4]^{2+}$ ion in HMPA, 5.17 Å, supports this deduction. If the solvated Cu²⁺ ion is either square planar or tetragonal in HMPA, the Stokes radius would be larger than 5 Å expected from the tetrahedral configuration. This problem has been discussed at the previous section on the solvated Ni²⁺ ion.

Configurations of Solvated Fe²⁺, Mn²⁺, and Zn²⁺ Ions in HMPA.

The values of log ϵ of solvated Fe²⁺ and Mn²⁺ ions in HMPA are 2.6 at 400 nm and –0.002 at 412 nm, respectively, while those of $[\text{Fe}(\text{hmpa})_4]^{2+}$ and $[\text{Mn}(\text{hmpa})_4]^{2+}$ in nitromethane are 2.6 and –0.002 at the same wavelengths, respectively. These values agree with those of the tetrahedral $[\text{Fe}(\text{hmpa})_4]^{2+}$ and the tetrahedral $[\text{Mn}(\text{hmpa})_4]^{2+}$ ions in nitromethane reported by Donoghue and Drago.³⁾ Therefore, it is concluded that solvated Fe²⁺ and Mn²⁺ ions in HMPA are $[\text{Fe}(\text{hmpa})_4]^{2+}$ and $[\text{Mn}(\text{hmpa})_4]^{2+}$ ions. Stokes radii of solvated Fe²⁺ and Mn²⁺ ions in HMPA are 5.00 Å and 5.47 Å, respectively (Table 1), suggesting

that they are both tetrahedral.

The configuration of solvated Zn^{2+} ion in HMPA can not be decided from the absorption spectrum. The Stokes radius of solvated Zn^{2+} ion in HMPA is 7.5 Å which is 2.5 Å larger than 5 Å expected for the tetrahedral configuration. Consequently, solvated Zn^{2+} ion in HMPA is probably octahedral. This is supported by the complex formation constants of Zn^{2+} ion with HMPA and with bpy; the details on this point will be published later.

General Discussion. Complexes of the first transition metal ions $[\text{M}^{\text{II}}(\text{hmpa})_4](\text{ClO}_4)_2$ ($\text{M}^{\text{II}} = \text{Mn}^{\text{II}}, \text{Fe}^{\text{II}}, \text{Co}^{\text{II}}, \text{Ni}^{\text{II}}, \text{Cu}^{\text{II}}, \text{or } \text{Zn}^{\text{II}}$) are tetrahedral in nitromethane except for $\text{Ni}(\text{II})$ and $\text{Cu}(\text{II})$ complexes, although they are all known to be tetrahedral in the solid states.^{2,3,5} In HMPA, the $\text{Mn}(\text{II})$, $\text{Fe}(\text{II})$, $\text{Co}(\text{II})$, and $\text{Cu}(\text{II})$ ions are tetrahedrally solvated by HMPA, while $\text{Ni}(\text{II})$ establishes equilibria among solvated complexes of the octahedral, square planar and tetrahedral configurations. $\text{Zn}(\text{II})$ forms probably an octahedrally solvated complex.

In dimethyl sulfoxide (DMSO) and *N,N*-dimethylformamide (DMF), solvated complex ions of the first transition metals are mostly octahedral. Since an HMPA molecule is very bulky as compared with DMSO and DMF, it seems that solvated complex ions in HMPA prefer the tetrahedral configurations to the octahedral ones.

Although Libuś and Uruska describe that the first transition metal complexes tend to be tetrahedral in solutions according to the differences between the crystal field stabilization energies (c.f.s.e.) of the octahedral and the tetrahedral configurations in the following order: $\text{Mn}(\text{II}) \sim \text{Zn}(\text{II}) > \text{Fe}(\text{II}) > \text{Co}(\text{II}) > \text{Cu}(\text{II}) > \text{Ni}(\text{II})$,¹⁶ $\text{Zn}(\text{II})$ prefers the octahedral configura-

tion in HMPA. Since $\text{Zn}(\text{II})$ has no c.f.s.e. in its complexes, it may be better to put it at the last in the sequence in the present case.

References

- 1) M. W. G. De Bolster and W. L. Groeneveld, *Recl. Trav. Chim. Pays-Bas*, **90**, 477 (1971).
- 2) J. T. Donoghue and R. S. Drago, *Inorg. Chem.*, **1**, 866 (1962).
- 3) J. T. Donoghue and R. S. Drago, *Inorg. Chem.*, **2**, 1158 (1963).
- 4) J. T. Donoghue and R. S. Drago, *Inorg. Chem.*, **2**, 572 (1963).
- 5) B. B. Wayland and R. S. Drago, *J. Am. Chem. Soc.*, **87**, 2372 (1965).
- 6) V. Gutmann, A. Weisz, and W. Kerber, *Monatsh. Chem.*, **100**, 2096 (1969).
- 7) "Japanese Industrial Standards; Testing Methods for Industrial Waste Water," ed by M. Tahara, Japanese Standards Association, Tokyo (1974), pp. 113 and 136.
- 8) G. Muto, "Hishoku Bunseki-ho," Kyoritsu Shuppan, Tokyo (1952), Chap. 8.
- 9) C. Atlani, J. C. Justice, M. Quintin, and J. E. Dubois, *J. Chim. Phys.*, **66**, 180 (1969).
- 10) T. Fujinaga, K. Izutsu, and S. Sakura, *Nippon Kagaku Zasshi*, **1973**, 191.
- 11) T. Fujinaga and S. Sakura, *Nippon Kagaku Zasshi*, **1977**, 135.
- 12) A. B. P. Lever, "Inorganic Electronic Spectroscopy," Elsevier Publishing Company, Amsterdam (1968), Chap. 9.
- 13) N. Iwasaki, K. Sone, and Y. Fukuda, *Z. Anorg. Allg. Chem.*, **412**, 170 (1975).
- 14) E. Bannister and F. A. Cotton, *J. Chem. Soc.*, **1960**, 1878.
- 15) A. D. Liehr, *J. Phys. Chem.*, **64**, 43 (1960).
- 16) W. Libuś and I. Uruska, *Inorg. Chem.*, **5**, 256 (1966).